NASA-CR-198613

Compression Strength of Composite Primary Structural Components

p. 6

Semiannual Status Report

Eric R. Johnson
Principal Investigator

Performance Period: November 1, 1994 to April 30, 1995

NASA Grant NAG-1-537

Aerospace and Ocean Engineering Department
Virginia Polytechnic Institute and State University
Blacksburg, Virginia 24061-0203

May, 1995

Technical Monitor: Dr. James H. Starnes, Jr., Head
Structural Mechanics Branch
National Aeronautics and Space Administration
Langley Research Center
Hampton, Virginia 23681-0001

(NASA-CR-198613) COMPRESSION STRENGTH OF COMPOSITE PRIMARY STRUCTURAL COMPONENTS Semiannual Status Report, 1 Nov. 1994 - 30 Apr. 1995 (Virginia Polytechnic Inst. and State Univ.) 6 p

N95-71245

Unclas

Z9/24 0049972

INTRODUCTION

Research continued on *Pressure Pillowing of an Orthogonally Stiffened Cylindrical Shell.* The motivation for this project is the planned utilization of advanced composite materials in the fuselage for large transport aircraft. In particular, the focus of this activity is the effect of cabin pressurization on the stiffener-to-skin joint. The design of stiffener-to-skin joints is one of the major technology issues in utilizing graphite/epoxy composites in the fuselage of a large transport aircraft. The manner in which the loads are transferred in the stiffener-to-skin joints under internal pressurization is important for determining the load capacity of these joints.

The objective of this project is to develop analyses of an orthogonally stiffened composite cylindrical shell subjected to internal pressure. These analyses are used to study the distribution of the interacting loads between the shell and stiffeners, and to study the pillowing of the shell, for a geometry and pressure typical of a large transport aircraft. Primarily the aim is to understand the fundamental mechanics of the load transfer in the vicinity of the shell-ring-stringer joint. Secondly, these analyses can be used in parametric studies of joint response, and perhaps for design. A potential benefit of such an analysis/design capability is to use fewer expensive fasteners in the graphite/epoxy fuselage. Where fasteners are required in a graphite/epoxy structure, aluminium fasteners cannot be used because of galvanic corrosion to the metal. More expensive fasteners, like titanium, are required to avoid corrosion.

RESEARCH ACCOMPLISHED

Work concluded on the effect of a ring, or frame, with an asymmetrical open cross section on the response of the structural repeating unit subject to uniform internal pressure. See Fig. 1. A ring with an asymmetrical cross section twists and bends out-of-plane under the internal pressure load in addition to bending in its plane and stretching along its circumference. Only symmetry about the x-axis for the repeating unit shown in Fig. 1 is preserved since the stringer cross section is assumed to be symmetric.

The major new feature incorporated into the analysis is the warping deformation of the ring's cross section due to torsion. This warping deformation is in addition to a previous extension of the model to include deformations due to transverse shear in the stiffeners and in the shell. Numerical data used in the analyses are representative of a large transport aircraft. (The shell radius is 122.0 inches, ring spacing is 22.0 inches, and the stringer spacing is 15.0 inches. The shell wall is a 13-ply $[\pm45, 90, 0, \pm60, 90, \pm60, 0, 90, \pm45]_T$ laminate of graphite-epoxy AS4/938 tow prepreg with a total wall thickness of 0.0962 inches. The stringer is an inverted hat section laminated from twelve plies of AS4/938 graphite-epoxy tow prepreg with a $[\pm45, 0_2, 90, \pm15, 90, 0_2, \pm45]_T$ layup with a total wall thickness of 0.0888 inches. The ring is 2-D braided graphite-epoxy J-section consisting of 0° and 90° tows with a wall thickness of 0.141 inches. The internal pressure p is 10 psi, and the Fourier Series for the displacements and interacting load intensities are truncated at 24 terms in the axial and circumferential directions.) Inclusion of warping was found to significantly change the response of certain interacting load components, joint rotations, and ring actions, as summarized below.

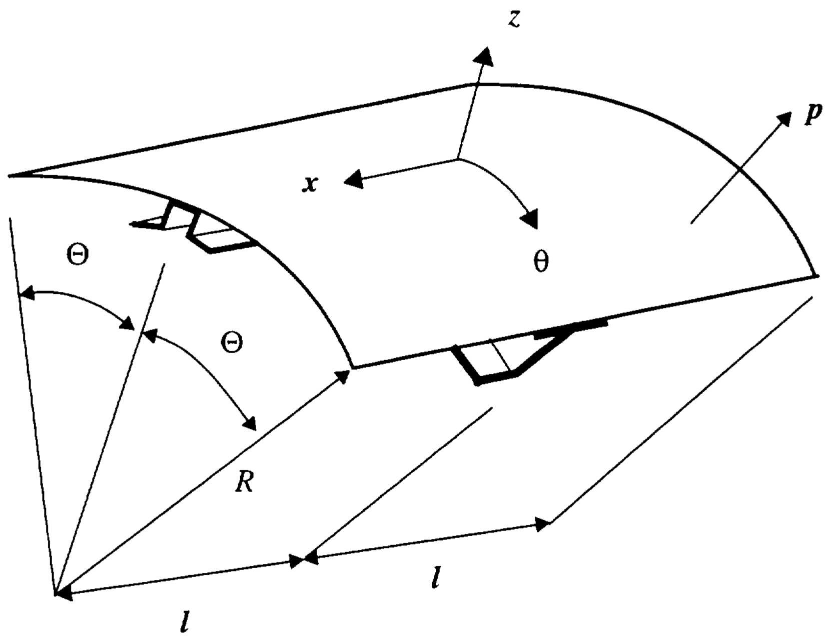

Fig. 1 Structural repeating unit of an orthogonally stiffened cylindrical shell subjected to a internal pressure *p*.

Interacting Load Distributions

There are two interacting line force components between the stringer and shell, and they are labeled λ_{xs} and λ_{zs} in Fig. 2. Between the ring and the shell there are three interacting force components labeled λ_{xr}, $\lambda_{\theta r}$, and λ_{zr} in Fig. 2, and, in addition, there are two line moment components $\Lambda_{\theta r}$ and Λ_{zr}. These line load intensities are continuously distributed along the contact lines between the attachment flanges, or faying flanges, of the stiffeners and the inside wall of the shell. As a point of reference, if both stiffeners have symmetric cross sections the response is symmetric about both the x- and θ- axes and then the interacting load components λ_{xr}, $\Lambda_{\theta r}$, and Λ_{zr} vanish.

The normal traction (dimensional units of F/L^2) between the ring's attachment flange and the shell wall is represented in the analysis by line force resultant λ_{zr} and line moment resultant $\Lambda_{\theta r}$. Line force intensity λ_{zr} represents the integral across the width of the attachment flange of the normal traction at any circumferential location, and the line moment intensity $\Lambda_{\theta r}$ represents the first moment of this traction integrated across the width of the attachment flange at any circumferential location. Both the $\lambda_{zr}(\theta)$ and $\Lambda_{\theta r}(\theta)$ distributions are symmetric about the joint, attaining maximum magnitudes at the joint, and have much smaller magnitudes away from the joint. (The joint is at $\theta = 0$.) At the joint, the sense of $\Lambda_{\theta r}$ is changed by the inclusion of warping deformation into the model, and additionally its magnitude is reduced by the inclusion of transverse shear

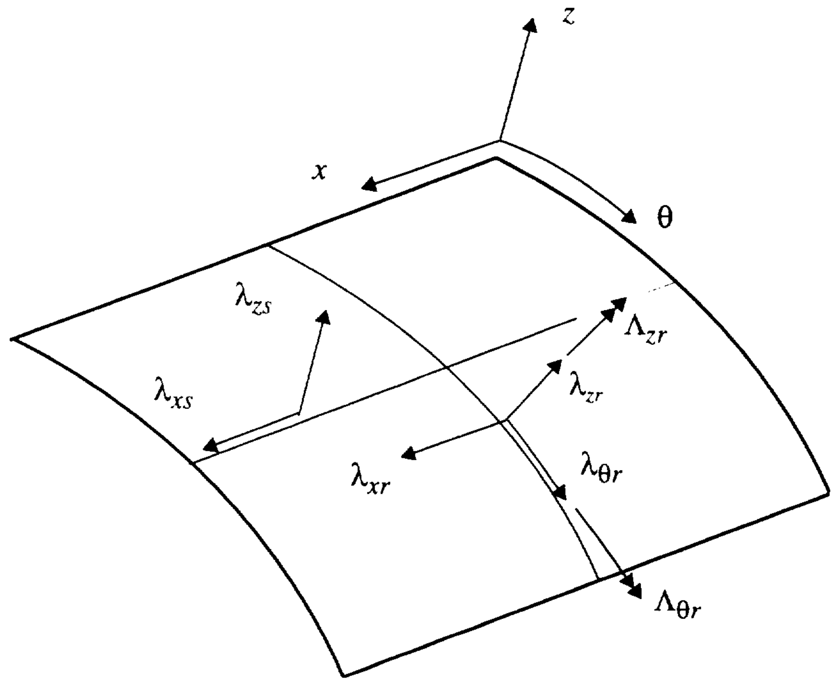

Fig. 2 Interacting line load intensities shown in the positive sense acting on the inside surface of the shell.

deformations. However, the force intensity λ_{zr} is essentially unaffected by the change in structural models. Thus, the transfer of the normal traction between the ring and shell is concentrated at the joint with the antisymmetric component of the distribution across the width of the attachment flange changing sign due to the inclusion of warping deformation of the ring into the structural model.

The distribution of the axial line load intensity $\lambda_{xr}(\theta)$ between the ring and shell is symmetric about the joint attaining a maximum magnitude at the joint, and has much smaller magnitudes away from the joint. Component λ_{xr} is increased by the inclusion of warping into the analysis and is reduced by the inclusion of transverse shear deformation. Thus, the maximum value of λ_{xr} is strongly influenced by warping and weakly influenced by transverse shear deformation.

The circumferential traction between the ring's attachment flange and the shell wall is represented in the analysis by line force resultant $\lambda_{\theta r}$ and line moment resultant Λ_{zr}. Line force intensity $\lambda_{\theta r}$ represents the integral across the width of the attachment flange of the circumferential traction, and the line moment intensity Λ_{zr} represents the first moment of this traction component integrated across the width of the attachment flange. Both the $\lambda_{\theta r}(\theta)$ and $\Lambda_{zr}(\theta)$ distributions are antisymmetric about the joint, attaining maximum magnitudes near the joint. The results for the Λ_{zr} distributions show the antisymmetric component in the distribution of the circumferential traction across the width of the ring's attachment flange is reversed, and its peak magnitudes are reduced, by the inclusion of warping deformations into the model. However, the magnitude of the line force intensity $\lambda_{\theta r}$ is only moderately affected by the change in structural models. Thus, the

major transfer of the circumferential traction between the ring and shell occurs close to the joint with the antisymmetric component of the distribution across the width of the attachment flange changing sign due to the inclusion of warping deformation of the ring into the structural model.

Joint Rotations

Rotations of the structural elements at the joint are shown in Fig. 3. The senses of the rotations

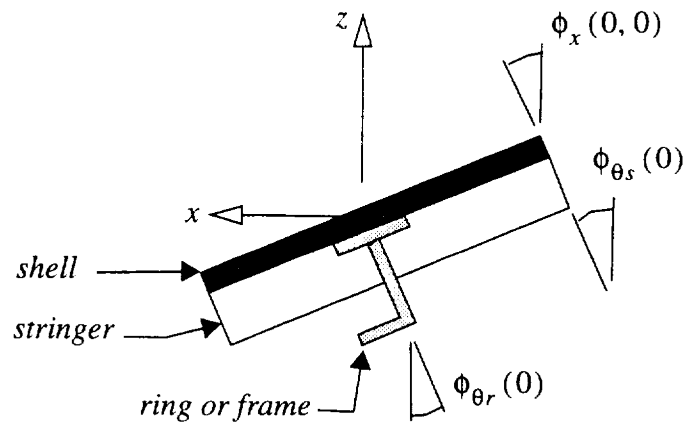

(a) $\phi_x(0,0) = \phi_{xs}(0) = \phi_{\theta r}(0)$

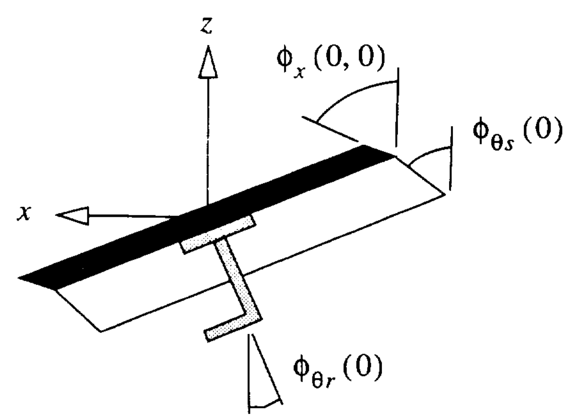

(b) $\phi_x(0,0) \neq \phi_{\theta s}(0) \neq \phi_{\theta r}(0)$

Fig. 3 Joint rotations for (a) the classical structural models, and (b) for transverse shear deformable models.

of the structural elements at the joint are changed with the inclusion of warping deformation in the ring as is shown in the Table 1. Also, as can be seen from the data in this table, the twist rotation of the ring at the joint increases by 40% with the inclusion of transverse shear deformation. That is, joint flexibility increases since element rotations at the joint are de-coupled by using transverse

shear deformation models.

Table 1: Rotations About The Circumferential Axis At The Stiffener Intersection.

Description of the Rotation of the Structural Component	Rotations in 10^{-5} radians			
	Classical Theory		Transverse Shear Theory	
	No Warping	Warping	No Warping	Warping
Shell normal $\phi_x(0, 0)$	- 2.56	2.58	-1.06	2.65
Ring twist $\phi_{\theta r}(0)$	- 2.56	2.58	-2.67	3.64
Stringer normal $\phi_{\theta s}(0)$	- 2.56	2.58	-0.29	1.85

Ring Actions

The out-of-plane bending moment and torque in the ring are very sensitive to the structural modeling. The distribution of the out-of-plane bending moment is symmetric about the joint, and the distribution of the torque is anti-symmetric about the joint. The total torque is the sum the warping torque, or Vlasov torque, and the St. Venant torque. Analyses neglecting warping show that the St. Venant torque is negligible compared to the warping component of the total torque. Warping torque is dominant because the continuous contact between the ring and shell restrains the cross-sectional warping of the ring. The out-of-plane bending moment is maximum at the joint, and this maximum increases due to inclusion of warping deformations into the model and decreases only a small amount due the inclusion of transverse shear deformations. The maximum magnitudes of total torque occur near the joint and decrease in value due the inclusion of transverse shear deformations into the model.

PUBLICATIONS

A conference paper was written on the details of the response of the structural repeating unit summarized above. The citation for this conference paper is

> Rastogi, N., and Johnson, E.R., "Analysis of an Internally Pressurized Orthogonally Stiffened Cylindrical Shell with an Asymmetrical Section Ring," Proceedings of *The 36th AIAA/ASME/ASCE/AHS/ASC Structures, Structural Dynamics and Materials Conference*, (New Orleans, LA, April 10-12, 1995), Part 3, AIAA, Washington, DC, pp. 1734-1759 (AIAA Paper No. 95-1368).

In addition, at this 36th SDM conference a poster was presented in the *Interactive Plenary Session* (3:30 pm –5:00pm, Tuesday April 11, 1995) for the paper cited above.

A report has been written on all the pressure pillowing research done under the grant for the performance period of November 1, 1991 to April 30, 1995. The citation for this report is

> Johnson, E.R., and Rastogi, N., "Load Transfer in the Stiffener-to-Skin Joints of a Pressurized Fuselage," College of Engineering, Virginia Polytechnic Institute and State University, Blacksburg, Virginia 24061, Report VPI-E-95-01, May 1995.